Self-Assembly

DOI: 10.1002/anie.200805202

Economical Design in Noncovalent Nanoscale Synthesis: Diverse Photofunctional Nanostructures Based on a Single Covalent Building Block**

*Galina Golubkov, Haim Weissman, Elijah Shirman, Sharon G. Wolf, Iddo Pinkas, and Boris Rybtchinski**

Noncovalent synthesis is an efficient "bottom-up" methodology for the construction of organic nanoscale systems by the self-assembly of covalent molecular building blocks.[1–3] The design of noncovalent systems takes advantage of encoding complexity in an economical way: a simple construction unit elicits the structure and function of the extended supramolecular arrays. This methodology can be further enhanced if a single generic covalent building block can be utilized for many structural and functional motifs; such a "molecular economy" approach being analogous to biological systems. The economical design of organic nanostructures has therefore attracted much interest[3–7] as it can further reduce the need of time-consuming covalent synthesis, and thus facilitates the screening and optimization of organic nanoscale systems. Herein we report the assembly of nanoscale ribbons, vesicles, tubes, and platelets, all based on a single generic covalent building block. Such diversity is achieved by using a two-stage self-assembly motif that is conveniently regulated through metal coordination. The nanostructures show good exciton mobility and can be utilized as light-harvesting systems.

Efficient generation of diverse nanostructures based on a single covalent building block requires a built-in functionality that can be expediently modified, which leads to changes in overall structure. By utilizing this concept, we have recently shown that the supramolecular fibers based on amphiphilic perylene diimide (PDI) units can undergo depolymerization (micelle formation) upon chemical reduction of PDIs, while oxidation with air restores the fibers.[8] This represents an interesting example of reversible supramolecular depolymerization, yet it is based on a single type of input—the reduction of a PDI unit. To achieve a high degree of diversity, a system that allows multiple inputs is required. Consequently, we aimed to introduce two levels of self-assembly encoding in a covalent building block: a general permanent self-assembly motif, and a tunable motif that has a broad range of possible modifications. We also aimed to produce a system in which self-assembly brings about useful photofunction. In pursuit of this idea, compound **1** (Scheme 1), our primary building block, was designed to possess an amphiphilic photoactive moiety and a ligand that is capable of binding a wide variety of metal centers (a unit for tuning). Thus, **1** consists of three principal components that are covalently linked: The strongly hydrophobic PDI chromophore (photofunctional unit), a hydrophilic polyethylene glycol (PEG) group, and the terpyridine (terpy) as a metal-coordinating moiety (the syntheses and characterization of compounds **1**–**4** are described in the Supporting Information). PEGylated amphiphilic PDIs are very advantageous self-assembling units because of strong hydrophobic interactions between PDI cores in aqueous medium.[7,9,10]

In a water/THF mixture (9:1 v/v), compound **1** self-assembles into long fibers (Figure 1a) as evidenced by cryogenic transmission electron microscopy (cryo-TEM). The fibers show a ribbonlike structure, and an occasional twisting of the ribbons from their narrower, high-contrast edges ((4 ± 0.6) nm) to their wider, low-contrast faces ((7.9 ± 1.3) nm) is observed (Figure 1a, white arrows). The length of the fibers is difficult to estimate as their end caps cannot be identified. Most of the fibers appear to extend over the entire cryo-TEM image and probably reach several microns in length.

The aligned, tightly packed fibers exhibit a fiber-to-fiber spacing of (7.1 ± 0.8) nm (Figure 1a), which corresponds to a high-contrast ordered aromatic core (responsible for fiber images in cryo-TEM) and low-contrast solvated PEGs (interfiber area). Individual fibers show a segmented structure (see inset in Figure 1a), such hierarchical structures with segmented cores are uncommon.[11,12] Notably, the 1.9 nm segment periodicity is almost identical throughout all structures and corresponds well to the dimensions of the PDI. A

[*] Dr. G. Golubkov, Dr. H. Weissman, E. Shirman, Dr. B. Rybtchinski
Department of Organic Chemistry
Weizmann Institute of Science, Rehovot 76100 (Israel)
Fax: (+972) 8-934-4142
E-mail: boris.rybtchinski@weizmann.ac.il
Homepage: http://www.weizmann.ac.il/oc/boris/
Dr. I. Pinkas
Department of Plant Sciences
Weizmann Institute of Science (Israel)
Dr. S. G. Wolf
Department of Chemical Research Support
Weizmann Institute of Science (Israel)

[**] This work was supported by grants from the Israel Science Foundation (grant no. 917/06) and the Helen and Martin Kimmel Center for Molecular Design. The cryo-TEM studies were conducted at the Irving and Cherna Moskowitz Center for Nano and Bio-Nano Imaging (Weizmann Institute). Transient absorption studies were performed at the Dr. J. Trachtenberg Laboratory for Photobiology and Photobiotechnology (Weizmann Institute) and were supported by a grant from S. Zuckermanof (Toronto, Canada). We thank Prof. R. Neumann for the access to modeling software. B.R. holds the Abraham and Jennie Fialkow Career Development Chair.

Supporting information for this article is available on the WWW under http://dx.doi.org/10.1002/anie.200805202.

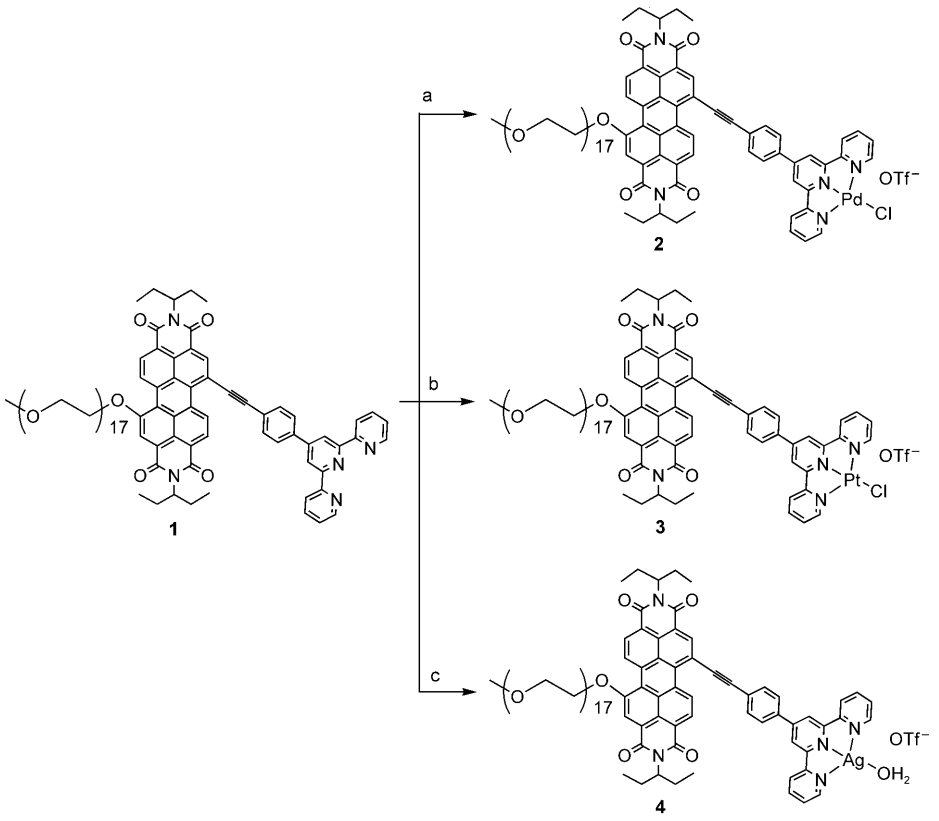

Scheme 1. Complexation of **1** with various metal centers. a) $[Pd(MeCN)_3Cl]OTf$, b) $[Pt(MeCN)_3Cl]OTf$, and c) AgOTf.

possible structure of the fibers is presented in Figure 1b (all schematic structures are based on molecular modeling studies, see the Supporting Information for details). We have observed a similar motif for an amphiphilic PDI system that possesses twofold symmetry.[8] Comparison of the UV/Vis spectra of assembled and disassembled **1** (Figure 1c) shows that self-assembly causes changes in the $0\rightarrow0$ and $0\rightarrow1$ transition intensities and substantial broadening of the spectrum. The complete inversion of $0\rightarrow0$ and $0\rightarrow1$ transition intensities is typical for face-to-face stacking (H aggregation) of PDIs.[13] A lesser degree of inversion in the case for **1** may be due to a less significant overlap of PDI aromatic systems or structural inhomogeneity in the fibers.

Pd, Pt, and Ag metal centers were chosen to modify the assemblies as the reaction of terpy with these metals gives square planar complexes.[14] The similar geometries of the complexes should allow a better insight into metal-dependent modification of nanoscale systems. Coordination of Pd, Pt, and Ag metal centers to **1** resulted in complexes **2**–**4** (Scheme 1).

In a water/THF mixture (9:1 v/v), compound **2** self-assembles into fiberlike structures, as evidenced by cryo-TEM (Figure 2a). The different contrast of the periphery and center of these structures is characteristic of the projection images of tubular aggregates (hollow cylinders). The nanotubes show a uniform diameter of (4.7 ± 0.4) nm and the internal diameter and the wall thickness are (1.1 ± 0.2) nm and (1.8 ± 0.2) nm, respectively. Similar to **1**, the length of the nanotubes is difficult to estimate, while most of them appear to extend over the entire cryo-TEM image and probably reach several microns in length. Comparison of the UV/Vis spectra of the aggregated and the disaggregated **2** (see Figure 2c) reveals an inversion of $0\rightarrow0$ and $0\rightarrow1$ transition intensities and significant broadening, which is typical of extended PDI assemblies with predominant face-to-face stacking (H aggregation). The possible structure of the tube is presented in Figure 2b. In this model, PEG groups are located at the periphery of the tube and cationic Pd centers cover the inner part. Notably, extended supramolecular nanotubes based on transition metal complexes are rare.[15,16]

Cryo-TEM images of compound **3** in a water/THF mixture (9:1 v/v) show mostly vesicular aggregates. The average diameter of the vesicles is 26 nm (Figure 3a) and the largest vesicle has a diameter of 72 nm. As vesicles are formed from bilayers that are closed on themselves, **3** is characterized by a self-assembly motif that is very different from that of the isoelectronic Pd complex **2**. The structure of the bilayer of **3** is most probably similar to that of **4** (Figure 4b).

A comparison of the UV/Vis spectra of the aggregated and the disaggregated **3** (Figure 3b) reveals a very significant broadening, a change in the vibronic bands intensity of PDI peaks, and a red shift of terpyridine platinum complex (terpyPt) band, which indicates that, besides strong interactions between PDIs, electronic coupling between terpyPt units is substantial. This is consistent with the known propensity of Pt–terpy complexes to interact through Pt–Pt interactions in solution and the solid state,[17,18] which appears to be the reason for a difference in the self-assembly patterns of **2** and **3**.

In a water/THF mixture (9:1 v/v), compound **4** self-assembles into nanoplatelets, with average dimensions of 60×40 nm (Figure 4a). The fine structure of the platelets (see inset in Figure 4a) reveals an ordered "striped" pattern, which shows a periodicity of (1.85 ± 0.05) nm. The UV/Vis spectrum of the assembled **4** (Figure 4c) shows an inversion of the $0\rightarrow0$ and $0\rightarrow1$ transition intensities and significant broadening, which is consistent with the formation of extended structures with a face-to-face stacking (H aggregation) motif. A possible model is presented in Figure 4b. Molecular modeling studies (see the Supporting Information) suggest that hydrogen bonding between coordinated water molecules may contribute to the directionality and strength of

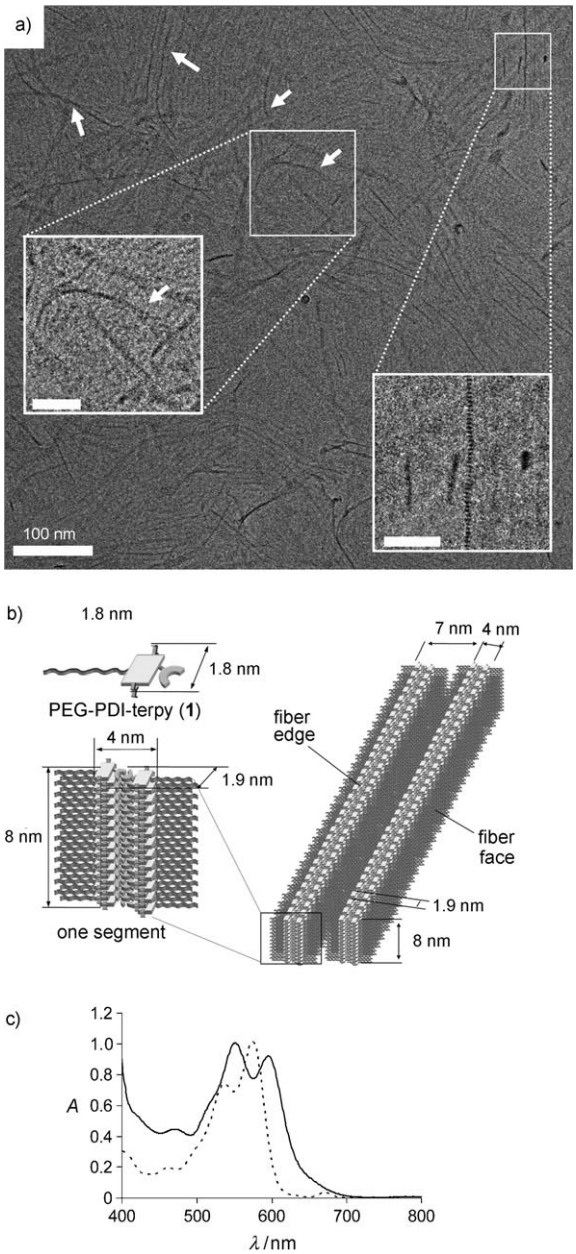

Figure 1. a) Cryo-TEM image of 2×10^{-4} M solution of **1** in a water/THF (9:1 v/v) mixture. The right inset shows an enlarged image of a segmented fiber (scale bar 40 nm) and the left inset shows an enlarged image of a fiber twist (scale bar 20 nm). The white arrows point at twisting regions (from the narrow edge to the wider face) of ribbonlike fibers (see Figure S12 in the Supporting Information for an enlargement of image (a)). b) Suggested structure of fibers of **1**. One fiber segment (which corresponds to the segment observed in cryo-TEM) and two aligned fibers are presented. The given dimensions are based on molecular modeling studies (see the Supporting Information). c) Normalized UV/Vis spectra of **1** in dichloromethane (disassembled, dotted line) and in water/THF (9:1 v/v) solution (solid line).

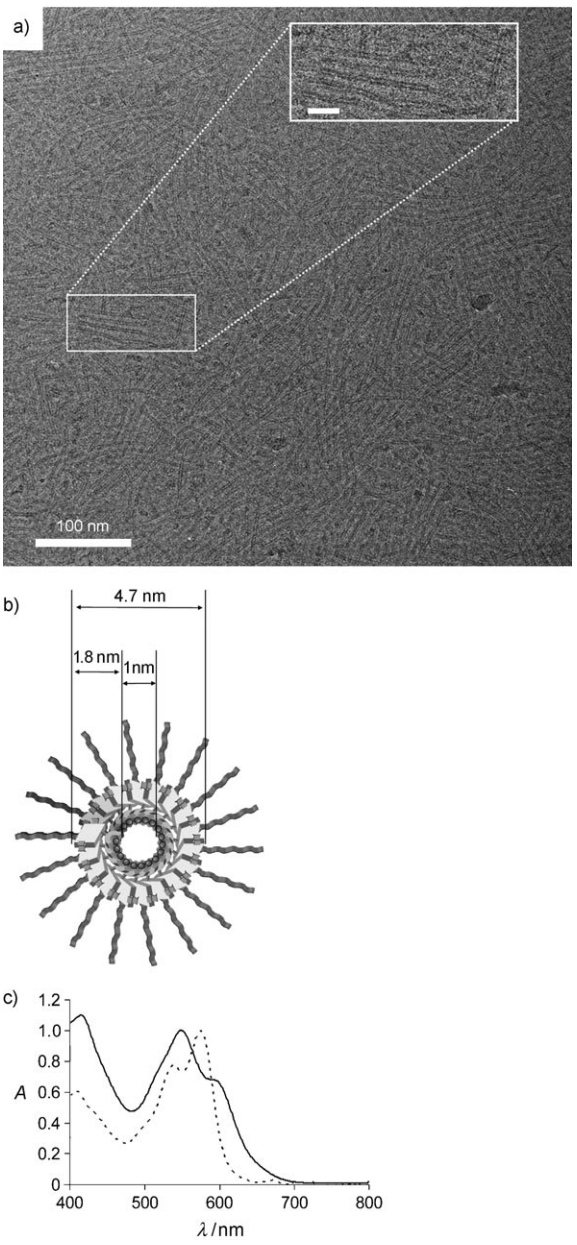

Figure 2. a) Cryo-TEM image of a solution of **2** (2×10^{-4} M) in water/THF (9:1 v/v). The inset shows an enlarged image of a nanotube (scale bar 20 nm). b) Suggested structure of the nanotubes (nanotube cross section; see Figure S13 in the Supporting Information for an enlargement of image (a)). c) Normalized UV/Vis spectra of a solution of **2** in dichloromethane (disassembled, dotted line) and in water/THF (9:1 v/v) solution (solid line).

the assembly, which results in a lower curvature of **4** (to give a more rigid assembly motif) than **2** and **3**.

Our systems strongly absorb visible light, while electronic interactions between the chromophore units in the assemblies are expected to promote efficient excitation energy transfer, which is pertinent to light harvesting. Femtosecond transient absorption studies on the nanostructures self-assembled from **1**–**3** (**4** was not sufficiently stable under laser light) reveal that the PDI excited-state feature shows multiexponential decay (Table 1). The contribution of the fast processes in the nanostructures is dependent on the laser power (in all cases, the relative amplitudes of τ_1 and τ_2 decrease with decreasing laser power, see Table 1). This result indicates that exciton annihilation takes place, which is typical of chromophore aggregates where a high photon flux of a laser pulse results in

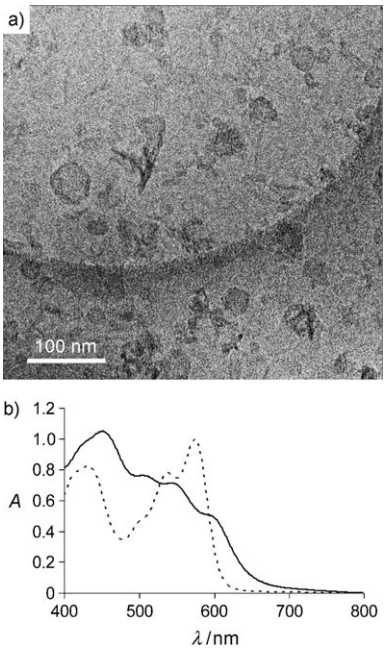

Figure 3. a) Cryo-TEM image of a solution of **3** (2×10^{-4} M) in water/THF (9:1 v/v). b) Normalized UV/Vis spectra of a solution of **3** in dichloromethane (disassembled, dotted line) and in water/THF (9:1 v/v) solution (solid line).

multiple excitations and enables exciton annihilation processes. Accordingly, disaggregated **1**–**3** (in chloroform solution) do not show power-dependent behavior. It should be noted that the presence of two power-dependent components may be attributed to the annihilation processes of delocalized (faster time) and localized excitons, as well as complex high-order multiexciton processes,[19] which complicate the elucidation of energy transfer patterns. By employing a widely used approximation, the site-to-site exciton hopping time constant, τ_{hop}, can be estimated from the annihilation time constant, τ_{an} (which corresponds to τ_1 and τ_2), by using an "exciton random walk" model that has been shown to give

Table 1: Time constants for the ^{1}*PDI decay (probed at 735 nm) at various pump fluences in water/THF (9:1 v/v) solution (relative amplitudes are given in parentheses).

		Pump fluences		
		2.26 mJ cm^{-2}	1.70 mJ cm^{-2}	1.10 mJ cm^{-2}
1	τ_1/ps	1.6 (0.46)	1.8 (0.41)	2 (0.37)
	τ_2/ps	45 (0.44)	45 (0.41)	45 (0.31)
	τ_3/ps	1160 (0.10)	1160 (0.16)	1160 (0.33)
2	τ_1/ps	4 (0.36)	4 (0.30)	4 (0.22)
	τ_2/ps	80 (0.55)	80 (0.55)	80 (0.49)
	τ_3/ps	1600 (0.09)	1600 (0.15)	1600 (0.29)
3	τ_1/ps	1 (0.30)	1 (0.18)	1 (0.14)
	τ_2/ps	20 (0.38)	20 (0.36)	20 (0.28)
	τ_3/ps	1400 (0.32)	1400 (0.46)	1400 (0.58)

satisfactory results for both natural and artificial chromophore aggregates.[20,21] According to this model, $\tau_{an} = (\pi^{-1}N\ln N + 0.2N - 0.12)\tau_{hop}$, where N is the number of hopping sites. In our experiments, the photon flux (the highest energy pulse) corresponds to one photon per six molecular units, which gives τ_{hop} values of 360 fs, 890 fs, and 220 fs (which correspond to τ_1) and 10 ps, 18 ps, and 4 ps (which correspond to τ_2) for **1**, **2**, and **3** respectively. For comparison, the hopping time constant observed for PDI aggregates in an organic medium is 5 ps.[21] Overall, good exciton mobility in the assemblies of **1**–**3** was observed. In-depth studies on the exciton dynamics in **1**–**3** are currently underway.

In conclusion, we have demonstrated that a single covalent generic building block can be used for the formation of diverse photofunctional self-assembled nanostructures such as ribbons, tubes, vesicles, and platelets. Such nanostructural diversity is achieved by using a design where noncovalent self-assembly is based on a two-level encoding—a permanent self-assembly motif that bears a unit capable of multiple "assembly controlling" inputs through metal coordination. The possibility to coordinate a wide variety of metal centers provides great latitude in structural control. Studies on the self-assembly of **1** regulated by coordination of various

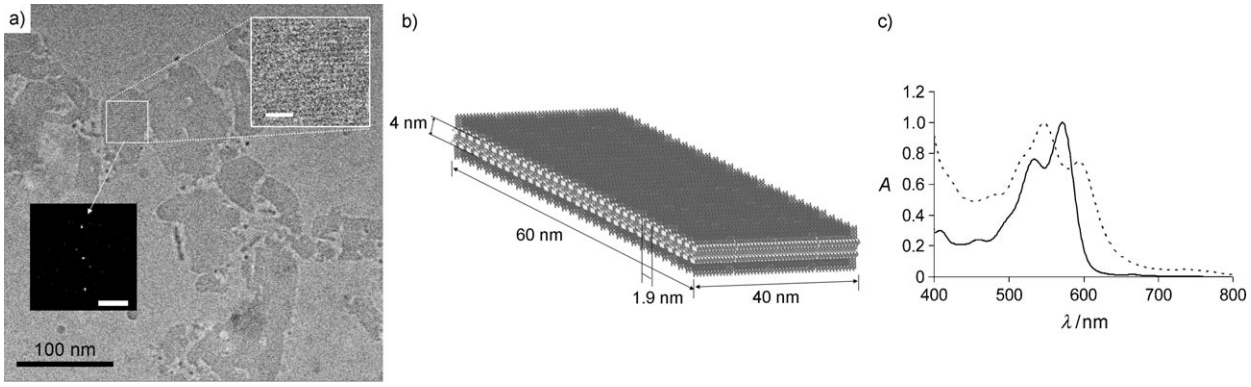

Figure 4. a) Cryo-TEM image of a solution of **4** (2×10^{-4} M) in water/THF (9:1 v/v). The inset surrounded by a white frame shows an enlarged image of a nanoplatelet (scale bar 10 nm) and the inset in a black square (scale bar 0.5 nm^{-1}) shows a fast Fourier transform image (performed on the region in the white frame), which shows high crystallinity with the pattern that corresponds to 1.85 nm spacing (see Figure S14 in the Supporting Information for an enlargement of image (a)). b) A model of the bilayer formed by **4**. c) Normalized UV/Vis spectra of a solution of **4** in dichloromethane (disassembled, dotted line) and in water/THF (9:1 v/v) solution (solid line).

metal centers and modification of their coordination sphere are currently underway.

Received: October 23, 2008

Keywords: aggregation · light harvesting · nanostructures · self-assembly · supramolecular chemistry

[1] G. M. Whitesides, B. Grzybowski, *Science* **2002**, *295*, 2418 – 2421.
[2] G. V. Oshovsky, D. N. Reinhoudt, W. Verboom, *Angew. Chem.* **2007**, *119*, 2418 – 2445; *Angew. Chem. Int. Ed.* **2007**, *46*, 2366 – 2393.
[3] J. M. Lehn, *Chem. Soc. Rev.* **2007**, *36*, 151 – 160.
[4] M. J. Mio, J. S. Moore, *MRS Bull.* **2000**, *25*, 36 – 41.
[5] J. A. A. W. Elemans, A. E. Rowan, R. J. M. Nolte, *J. Mater. Chem.* **2003**, *13*, 2661 – 2670.
[6] L. C. Palmer, Y. S. Velichko, M. Olvera de La Cruz, S. I. Stupp, *Philos. Trans. R. Soc. London Ser. A* **2007**, *365*, 1417 – 1433.
[7] J.-H. Ryu, D.-J. Hong, M. Lee, *Chem. Commun.* **2008**, 1043 – 1054.
[8] J. Baram, E. Shirman, N. Ben-Shitrit, A. Ustinov, H. Weissman, I. Pinkas, S. G. Wolf, B. Rybtchinski, *J. Am. Chem. Soc.* **2008**, *130*, 14966 – 14967.
[9] X. Zhang, Z. J. Chen, F. Würthner, *J. Am. Chem. Soc.* **2007**, *129*, 4886 – 4887.
[10] Y. K. Che, A. Datar, K. Balakrishnan, L. Zang, *J. Am. Chem. Soc.* **2007**, *129*, 7234 – 7235.
[11] Z. B. K. Li, Y. E. Talmon, M. A. Hillmyer, T. P. Lodge, *Science* **2004**, *306*, 98 – 101; Y. E. Talmon, M. A. Hillmyer, T. P. Lodge, *Science* **2004**, *306*, 98 – 101.
[12] H. G. Cui, Z. Y. Chen, S. Zhong, K. L. Wooley, D. J. Pochan, *Science* **2007**, *317*, 647 – 650.
[13] F. Würthner, *Chem. Commun.* **2004**, 1564 – 1579.
[14] S. Binsilong, J. D. Kildea, W. C. Patalinghug, B. W. Skelton, A. H. White, *Aust. J. Chem.* **1994**, *47*, 1545 – 1551.
[15] V. G. Organo, D. M. Rudkevich, *Chem. Commun.* **2007**, 3891 – 3899.
[16] T. Shimizu, M. Masuda, H. Minamikawa, *Chem. Rev.* **2005**, *105*, 1401 – 1443.
[17] A. Y.-Y. Tam, K. M.-C. Wong, G. Wang, V. W.-W. Yam, *Chem. Commun.* **2007**, 2028 – 2030.
[18] V. W.-W. Yam, K. M.-C. Wong, N. Zhu, *J. Am. Chem. Soc.* **2002**, *124*, 6506 – 6507.
[19] M. VanBurgel, D. A. Wiersma, K. Duppen, *J. Chem. Phys.* **1995**, *102*, 20 – 33.
[20] E. W. Montroll, *J. Math. Phys.* **1969**, *10*, 753 – 765.
[21] M. J. Ahrens, L. E. Sinks, B. Rybtchinski, W. H. Liu, B. A. Jones, J. M. Giaimo, A. V. Gusev, A. J. Goshe, D. M. Tiede, M. R. Wasielewski, *J. Am. Chem. Soc.* **2004**, *126*, 8284 – 8294.

